

germanium at 800°C, where several measurements were taken, fell between  $1 \times 10^{-13}$  and  $5 \times 10^{-12}$  cm<sup>2</sup>/sec. This value is several orders of magnitude smaller than that reported by Fuller in the accompanying letter and by Dunlap.<sup>2</sup> The activation energy for the process, which is calculated from the temperature dependence of the diffusion rate, is about 3.0 electron volts.

The limiting concentrations were calculated from conductivity measurements made locally on each side of the junction. The calculation employs the mobility of holes and electrons, and we have used Hall effect data obtained from Pearson and Debye<sup>3</sup> which include most of the range of impurity concentration in the junctions studied.

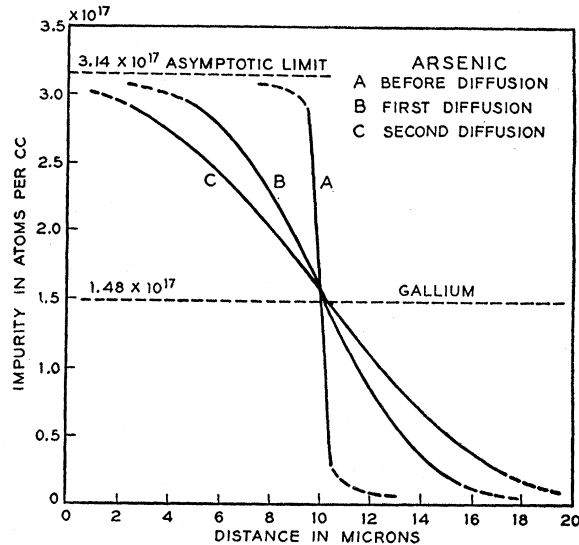


FIG. 2. Impurity concentration gradients in the region of the *p-n* junction as deduced from Fig. 1.

For all junctions the capacitance was found to be proportional to the inverse cube root of the bias voltage. This relationship is expected for junctions in which the gradient is constant across the transition region.<sup>1</sup> For one junction it was possible to observe a sharp Zener break<sup>4</sup> in the current-voltage curve at each step throughout the heat treatments. The concentration gradients obtained from the critical Zener voltages agreed to within 20 percent with those obtained from the capacitance measurements.

There are two features of the technique which make it particularly suitable for measurement of diffusion. First, it permits the significant measurement of very small diffusion distances and very low concentrations of impurities. Second, and perhaps more important, diffusion may be studied from a gradient which is established in the crystal at the time it is grown. In the usual techniques for measurement of diffusion in solids, the impurity atoms are introduced at the surface. Their concentration here is difficult to determine since it may be influenced by adsorption and chemical reactions. If the surface concentration builds up sufficiently, it may reach a composition which will melt at the temperature under investigation. In the method described here there is no reservoir of the impurity and no mechanism for its concentration to increase beyond that built into the crystal when it is grown.

We wish to acknowledge the assistance of Mr. R. M. Mikulyak in growing the crystals and of Miss C. J. Peffer in taking many of the measurements. Mr. W. van Roosbroeck obtained the particular solutions of the diffusion equation.

<sup>1</sup> W. Shockley, Bell System Tech. J. **28**, 335 (1949).

<sup>2</sup> W. C. Dunlap, Jr., Bull. Am. Phys. Soc. **27**, No. 1 (1952).

<sup>3</sup> G. L. Pearson and P. P. Debye, private communication.

<sup>4</sup> McAfee, Ryder, Shockley, and Sparks, Phys. Rev. **83**, 650 (1951).

## Pressure Broadening of Absorption Lines\*

GILBERT N. PLASS AND DOUGLAS WARNER  
The Johns Hopkins University, Baltimore, Maryland  
(Received January 21, 1952)

SPITZER<sup>1</sup> has shown that the familiar Lorentz formula for the absorption coefficient

$$k(\nu) = (S\alpha/\pi)[(\nu - \nu_0)^2 + \alpha^2]^{-1} \quad (1)$$

is valid when  $|\nu - \nu_0| < 3M^{-1}$ , where  $\alpha$  is the half-width of the line,  $\nu$  is expressed in wave numbers,  $S$  is the total intensity of the line,  $M = 27.8(c/\nu)^{6/5}b^{1/5}$ , and  $b$  is the constant in the frequency perturbation  $\nu_p(t) = b\nu^{-6}$ . Although the following calculations can be easily extended to perturbations varying as  $r^{-n}$ , we give only the results for Van der Waals forces.

Holstein<sup>2</sup> has shown that  $k(\nu)$  derived from statistical theories is valid at moderate pressures and for nondegenerate levels when  $|\nu - \nu_0| > 3M^{-1}$ . In this range of frequencies the Lindholm<sup>3</sup> equations are valid in the wings of the line

$$k(\nu) = (0.933)(M^2 S \alpha / \pi) [M(\nu_0 - \nu)]^{-3/2} \quad (2a)$$

and

$$k(\nu) = (0.638)(M^2 S \alpha / \pi) [M(\nu - \nu_0)]^{-7/3} \quad (2b)$$

In the usual case Eqs. (2a, b) apply to the red and violet wings, respectively. Instead of the discontinuous rectangular pulses used by Lindholm, Holstein,<sup>4</sup> using an inverse power frequency perturbation, obtains Eq. (2a) for the red wing and

$$k(\nu) = (16.6)(M^2 S \alpha / \pi)(\nu - \nu_0)^{-7/3} \times \exp\{- (0.474)[M(\nu - \nu_0)]^{5/6}\} \quad (2c)$$

for the violet wing. All of the calculations reported here have been made using both Eqs. (2b) and (2c). Although the latter equation is based on more reasonable physical assumptions, we find that the difference in the results calculated from these two equations does not differ by more than a few percent within the range of validity of the statistical theory. This is because the absorption from the red wing dominates the violet. Since Lindholm's equations are easier to integrate and give the same answers as Holstein's, we report below only on calculations made with Eqs. (2a, b).

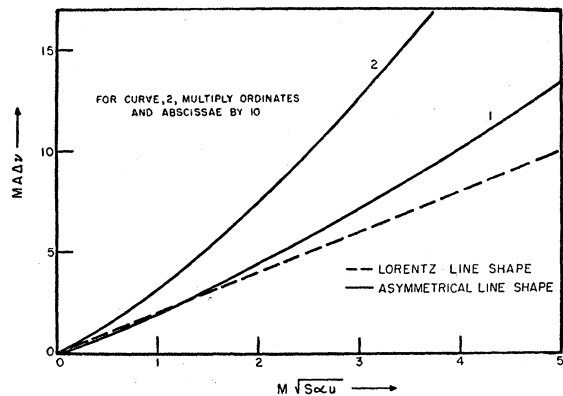


FIG. 1. Absorption of a single line as a function of  $M(Sau)^{1/2}$  [Eqs. (3) and (4)]. The dashed and solid lines show the absorption with the Lorentz and asymmetrical line shapes, respectively. Both the ordinates and abscissae of curve 2 should be multiplied by ten.

The fractional absorption,  $A$ , by a single line is given by the familiar square root law

$$A \Delta \nu = 2(Sau)^{1/2}, \quad (3)$$

when the radiation is completely absorbed at the center of the line, where  $u$  is the optical thickness of the absorbing gas. If  $k(\nu) \sim |\nu - \nu_0|^{-n}$  in the wings of the line, by the usual derivation  $A \sim (Sau)^{1/n}$ . For  $n=2$ , this agrees with Eq. (3). If  $k(\nu)$  is given

by Eqs. (2a, b), then

$$A \Delta \nu M = (1.19)(M^2 S \alpha u)^{2/3} + (0.789)(M^2 S \alpha u)^{3/7}. \quad (4)$$

Equation (3) is valid when there is little absorption from the beam for wave numbers  $|\nu - \nu_0| > 3M^{-1}$ . Equation (4) is valid when the beam is largely absorbed for all  $|\nu - \nu_0| < 3M^{-1}$ . When neither of these conditions is satisfied, the value of  $A$  is intermediate between that given by Eqs. (3) and (4). In Fig. 1, where these equations are plotted, it is seen that the actual absorption curve in this range is always concave upwards and thus could not be confused experimentally with the concave downwards curve that begins when the lines in a band begin to overlap. The stronger absorption from Eq. (4) than from (3) for large  $M^2 S \alpha u$  is due entirely to the larger  $k(\nu)$  in the red wing.

We have also calculated the transmission of an idealized band of equally spaced, equally intense lines with  $k(\nu)$  given by Eqs. (2a, b) by the same procedure used by Elsasser<sup>5</sup> for the Lorentz shape. In our case the calculations have to be performed numerically. The results are given in Fig. 2. The region of validity

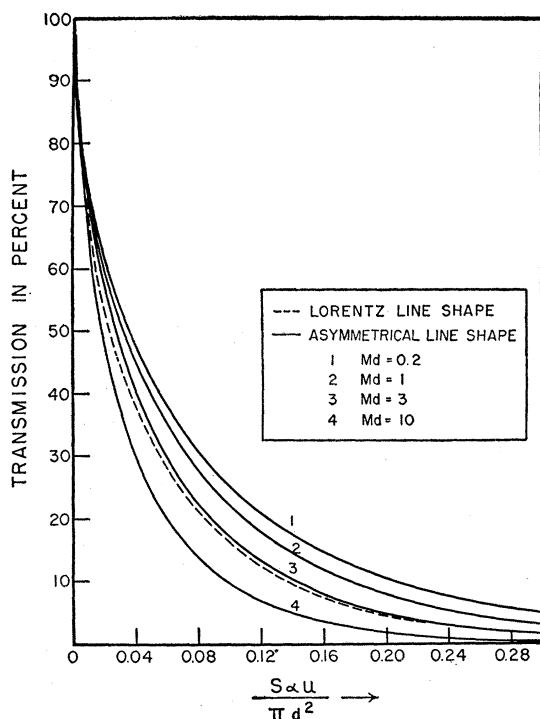


FIG. 2. Transmission of an idealized band as a function of  $S \alpha u / \pi d^2$ , where  $d$  is the separation between line centers in the band.

of these curves is determined by considerations similar to those for a single line. The curves for  $M d \leq 1$  should be modified by using  $k(\nu)$  from Eq. (1) for nearby lines and Eqs. (2a, b) for more distant lines.

An experimental measurement of the line shape in the wings by accurate measurement of the absorption of a single line would be desirable in view of the importance of this subject for band absorption and for considerations of heat transfer in the atmosphere.<sup>6</sup> A paper discussing these applications in detail will appear shortly in another journal.

\* This work was supported by the ONR.

<sup>1</sup> L. Spitzer, Jr., Phys. Rev. **58**, 348 (1940).

<sup>2</sup> T. Holstein, Phys. Rev. **79**, 744 (1950).

<sup>3</sup> E. Lindholm, Arkiv Mat. Astron. Fysik **32**, No. 17 (1946).

<sup>4</sup> T. Holstein, private communication.

<sup>5</sup> W. M. Elsasser, Phys. Rev. **54**, 126 (1938).

<sup>6</sup> J. Strong and G. N. Plass, Astrophys. J. **112**, 365 (1950); L. D. Kaplan, J. Met. (to be published).

## Interferometric Measurements of the Hyperfine Structure of the Mercury Green Line\*

JOHN STERNER

Baird Associates, Inc., Cambridge, Massachusetts

(Received January 7, 1952)

IN his classic work on the subject, Schüler<sup>1</sup> did not include accurate wavelength measurements of the six normally unresolved components which make up the main part of the green line of mercury. He did, however, from theoretical considerations predict accurately all the components which have been found, including an analysis of their separations.

Gehrcke and Lau,<sup>2</sup> followed by Burger and Van Cittert<sup>3</sup> using quite different techniques, measured all components. The values given by these authors checked reasonably well with Schüler's earlier measurements of the resolved components and predictions of the unresolved.

Recently, Breit<sup>4</sup> has pointed out the importance, for a better understanding of intranuclear forces, of more accurate measurements of hyperfine structure components. Mercury hyperfine structure has a particular significance in this respect because it has five even isotopes and two odd, thus offering an array of nuclear levels for studying and evaluating anomalous behavior.

In the present work previous measurements of the hyperfine structure of the green line of mercury have been refined by application of a novel Fabry-Perot interferometer which permits photographing of patterns rapidly and with high resolution. Each interferometer plate consists of a multilayer film formed by the alternate deposition of layers of two dissimilar dielectrics. The resultant film is similar to that which is deposited in the fabrication of the presently available commercial interference filters.<sup>5</sup> In this way a resolving power of nearly three million has been obtained using spacers of only 37 mm in a standard Fabry-Perot interferometer. Since absorption in a multilayer film is very much lower than that inherent in a silver film, transmission is considerably higher for equivalent reflecting power. Indeed, it has been possible to make high resolution interferograms in a matter of minutes, so quickly that only the crudest temperature regulation is required.

A typical interferogram is shown in Fig. 1. This was made by using an enriched isotope sample furnished by the Isotopes Division of the U. S. Atomic Energy Commission. The sample illustrated contains nearly equivalent amounts of Hg<sup>198</sup>, Hg<sup>200</sup>, Hg<sup>202</sup>, and Hg<sup>204</sup>. The components shown are approximately 0.03 cm<sup>-1</sup> apart.

In Table I are given measurements of the central components

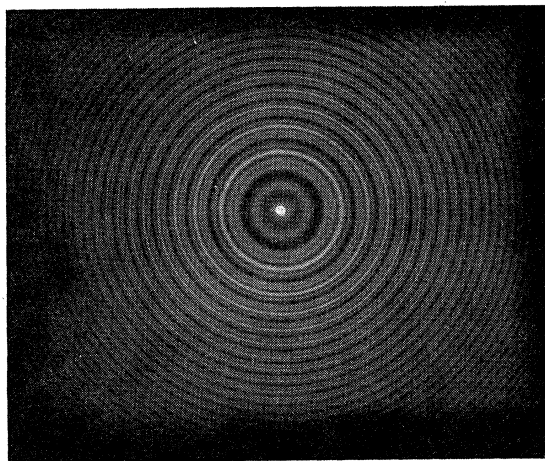


FIG. 1. A typical interferogram of the mercury green line, using an enriched isotope sample.